



Contents list available at IJRED website

International Journal of Renewable Energy Development

Journal homepage: <https://ijred.undip.ac.id>



Research Article

Adsorption method using zeolite to produce fuel-grade bioethanol

Hargono Hargono^{*}, Noer Abyor Handayani, Sheila Dwifa Andani, Ersya Wardani, Ulma Aqari Fisama, Kevin Setiadi Seng

Chemical Engineering Department, Faculty of Engineering, Diponegoro University, Semarang, Central Java, Indonesia

Abstract. Bitter cassava (*Manihot glaziovii*) has the potential to be converted into bioethanol. However, the distillation process can only purify it to 95% bioethanol. Therefore, it is necessary to carry out an adsorption process to obtain 99.8% bioethanol. This study aimed to investigate the effect of bitter cassava starch hydrolysis time and coral rock in the distillation column on glucose and bioethanol concentrations, respectively. Additionally, the study discussed the effect of adsorbent height (60, 80, 100, or 120 cm) in the adsorption column on bioethanol concentration. There are three main stages for obtaining fuel-grade bioethanol: (i) bitter cassava hydrolysis, (ii) bioethanol production, and (iii) bioethanol purification (distillation and adsorption). Zeolite 4A and natural zeolite were used as adsorbents in this study. The results showed that the best fermentation was obtained at 90 hours, resulting in an ethanol concentration of 13.82% (v/v), which could be purified up to 95.64% through distillation. Furthermore, further purification (adsorption) could extend fuel-grade bioethanol (99.62% and 98.42%). Another analysis also indicated that zeolite 4A was more feasible than natural zeolite for producing fuel-grade bioethanol.

Keywords: distillation, coral rock, adsorption, zeolite 4A, natural zeolite, bioethanol



© The author(s). Published by CBIORE. This is an open access article under the CC BY-SA license (<http://creativecommons.org/licenses/by-sa/4.0/>).

Received: 15th Dec 2022; Revised: 18th June 2023; Accepted: 17th July 2023; Available online: 25th July 2023

1. Introduction

Commonly, high population growth rates, rapid development of industry, and dependency on fossil fuels are the main reasons that contribute to the global energy crisis (Jambo *et al.*, 2016). The overconsumption of conventional fuel-based fossil fuel also leads to negative consequences, such as a lack of fuel reserves, an increase in commodity prices, pollution, and climate change (Suali & Sarbatly, 2012; Adenle *et al.*, 2013; Jambo *et al.*, 2016). Therefore, there is an urgent need for new renewable resources to produce sustainable energy, thus overcoming these challenges. Biodiesel and bioethanol are alternative biofuels that can be used to replace diesel and petrol, respectively (Ariyanti and Hadiyanto, 2013; Aditiya *et al.*, 2016). Numerous studies have been conducted on biodiesel production (Handayani *et al.*, 2013; Tabatabaei *et al.*, 2019; Mehdi *et al.*, 2022; Nazloo *et al.*, 2022).

The availability of continuous feedstock is one of the main factors that is important for bioethanol production and commercialisation (Ocreto *et al.*, 2021; Jambo *et al.*, 2016; Hadiyanto *et al.* 2013). Bioethanol can be produced from biomass feedstocks, which are natural sources of carbon that can be converted into bioenergy through biological treatment processes such as fermentation. Bitter cassava (*Manihot glaziovii*) is a plant that grows in tropical areas (Hargono *et al.*, 2017a), and it contains 88% starch, so it may be an appropriate commodity for bioethanol conversion (Hargono *et al.*, 2017b). The production of bioethanol consists of four (4) sequential steps: (i) pre-treatment, (ii) hydrolysis, (iii) fermentation, and (iv) separation-purification. Among these steps, separation is a crucial stage for bioethanol purification (Aditiya *et al.*, 2016). To

meet fuel-grade standards, the concentration of bioethanol should be higher than 99% (Lee *et al.*, 2021; Kusmiyati & Susanto, 2015; Muhaji & Sutjahjo, 2018). Therefore, it is necessary to carry out separation and purification processes to achieve the required ethanol concentration for fuel-grade bioethanol.

The fermentation process of sugar-based raw materials using *Saccharomyces cerevisiae* produces an ethanol-water mixture (Cardona & Sanchez, 2007; Hossain *et al.*, 2010). Then, the ethanol purification process can be conducted by distillation and adsorption. The distillation process can purify the ethanol concentration up to 94% due to the azeotropic point limitation (Kusmiyati & Susanto, 2015; Lei *et al.*, 2002). However, an adsorption process then needs to be carried out to obtain a higher concentration (> 99%) (Kusmiyati & Susanto, 2005). The adsorbent, as a molecular sieve, must have a selective pore size. For instance, water (H₂O) has a molecular diameter of 2.75 Å while ethanol (C₂H₅OH) has a molecular diameter of 4.40 Å (Perry & Green, 1997). The combination of distillation and adsorption is required to ensure that the bioethanol produced can meet the standard of fuel grade.

Adsorption is one of the most accessible purification techniques since the raw material for the adsorbent is very easy to obtain (Karimi *et al.*, 2019). Common adsorbent materials used in the purification of bioethanol include zeolite, silica sand, starch material, and activated carbon (Lee *et al.*, 2020). The porous properties of the adsorbent determine the efficiency of dehydration in the adsorptive process. Previous studies reported that the use of silica gel as an adsorbent could produce 98.28% ethanol (Mekala *et al.*, 2022). Other studies also

* Corresponding author

Email: hargono@che.undip.ac.id (H.Hargono)

explained that zeolite 3A and zeolite could purify ethanol at concentrations of 99.5% and 99.4%, respectively (Abdeen *et al.*, 2011; Handrian *et al.*, 2017). Since its great performance, zeolite has been well known as the best adsorbent and most efficient dehydrator of ethanol (Perry & Green, 1997). Zeolite-type molecular adsorbents can achieve high water selectivity, which can be made to be both size- and sorption-selective for water (Lee *et al.*, 2020). Due to the small diameter (0.275 nm), water molecules can easily pass through the zeolite channels compared to ethanol, which has a larger diameter (0.44 nm) (Mekala *et al.*, 2022). However, only a few researchers have highlighted the effect of different controlling parameters in the packed column system on the dehydration process. Hence, investigation of adsorbent heights in the adsorption column is urgently required to obtain fuel-grade bioethanol. This research aims to study the effect of bitter cassava starch hydrolysis time in the hydrolysis process and the use of coral rocks in the distillation process on glucose and bioethanol concentrations, respectively. Additionally, the effect of the adsorbent height in the adsorption column on bioethanol concentrations is also discussed in this paper.

2. Materials and Methods

2.1 Materials

Bitter cassava (*Manihot glaziovii*) was supplied from Ngepungsari village, Karanganyar, Central Jawa, Indonesia, and cassava starch production was carried out using the extraction method as described by previous work (Hargono *et al.*, 2017^a). Coral rock was obtained from Kampung Laut Cilacap, which is located on the edge of the Segara Anakan lagoon in Central Jawa.

2.2 Chemicals

Potassium sodium tartrate tetrahydrate and 3,5-Dinitrosalicylic acid (Merck), NaOH (98%, Merck), Na₂SO₃ (98.5%, Merck), H₂SO₄ (98.5%, Merck), sodium acetate buffer (Merck), glucose and ethanol (99.5%, Merck), (NH₄)₂HPO₄, MgSO₄·7H₂O, and yeast extract were purchased at Sigma-Aldrich Indonesia (Hargono *et al.*, 2017^b). Zeolite 4A was obtained from the Chemical Engineering Operations Laboratory, Faculty of Engineering, Diponegoro University, while natural zeolite was purchased at the Multi Kimia Raya Kimia, Semarang, Indonesia.

2.3 Enzyme

Granular Starch Hydrolysing Enzyme (GSHE), also known as Stargen™ 002, is a commercial enzyme obtained from Genencor International (USA) (Genencor, 2019). This enzyme (amylase and glucoamylase) contains *Aspergillus kawachii*, which was found in *T. reesei*. Both amylase and glucoamylase enzymes work synergistically to hydrolyze starch granules into glucose. The enzyme has an activity of 570 GAU/g and a pH of 4–4.5. The minimum activity of alpha-amylase is 135 KNUg⁻¹, and that of glucoamylase is 270 GAUg⁻¹. One glucoamylase unit (GAU) is defined as the number of enzymes that discharge 1 g of reducing sugar, measured as glucose, per hour from the dissolvable starch substrate under the conditions of the study (Hargono *et al.*, 2017^b).

2.4 Microorganism

Saccharomyces cereviceae, also known as baker's yeast, was produced by PT Pakmaya and obtained from Kabita Store, Semarang, Indonesia. The yeast was stored in a refrigerator

before use. *Saccharomyces cereviceae* was dispersed in clean water at room temperature at a concentration of 10 g/L (dry pastry yeast/ per litre of DI water), and 10 mL of this was used as inoculum without further cultivation and added to 90 mL of maturation medium to get a 10% (v/v) portion. Before being added, the cup and medium were sanitised by operating the autoclave at 121°C and 0,5 hours, respectively. The temperature and agitation speed were kept steady (Hargono *et al.*, 2019).

2.5 Starch hydrolysis: Non-cooking method

This study investigated the effect of cassava starch concentrations (100, 150, and 200 g/L) on glucose concentrations. Initially, the starch slurry was incubated in a shaker at 100 rpm for 10 minutes at pH 4.5. The pH was controlled using a sodium phosphate buffer solution (0.01 M) of citric acid. The cassava starch slurry was then transferred into a test jar for the hydrolysis process. Furthermore, the enzyme with a concentration of 1.5% (w/w) was added at 30°C, pH 4, for 24 hours (Hargono *et al.*, 2017^b). The samples were taken for periods of 6, 12, 18, and 24 hours and centrifuged for 4 minutes at a rotation speed of 100 Hz. The samples were filtered using Whatman CAT 40 filter paper No.1440–125 mm in order to obtain a clear filtrate, and then the filtrate was analysed to determine the concentration of glucose. The best result of this hydrolysis process is the concentration of substrate and enzyme that produces the maximum concentration of glucose. Furthermore, glucose produced in these best conditions is used as feed for the fermentation process to produce bioethanol.

2.6 Starch characterization

Native starch and hydrolyzed starch were characterised for their microstructure and crystalline phases. The microstructure of the starch granules was observed using a scanning electron microscope (JEOL Series, JSM-6510-LA, Japan) with an object magnification of 3000x. The crystallinity phase of starch granules was investigated through X-ray diffraction (XRD) pattern analysis.

2.7 Simultaneous saccharification and fermentation (SSF)

The SSF was carried out using a 1000-mL volume flask that had been sterilised at 121 °C for 30 minutes. The bitter cassava starch (200 g/L) was put into a flask at pH 5. pH adjustment was conducted using a 3 M NaOH solution. Stargen™ 002 (1.5% w/w) was then added at 50 °C for 24 hours, and then the system was maintained at 30 °C. Fermentation was carried out in the same flask by adding several nutrients: (NH₄)₂HPO₄ 0.5 g/L, MgSO₄·7 H₂O 0.025 g/L, and yeast extract 1.0 g/L for 15 hours in a shaker-incubator at 37 °C and 80 rpm. Furthermore, 5 g/L of dry yeast was added and incubated in anaerobic conditions for 78 hours. Samples were taken periodically for bioethanol concentration analysis at 6, 12, 18, and 78 hours.

2.8 Reduction of coral rock

Irregularly shaped coral rock was reduced using a hammer mill (Matsumoto, HM 9300) to become smaller in size with an average size of 1 cm, and then this material was filled in the distillation column.

2.9 Bioethanol purification using distillation and adsorption Methods

In this study, single-stage distillation and adsorption were used to purify bioethanol (Fig. 1). The crude bioethanol (1000

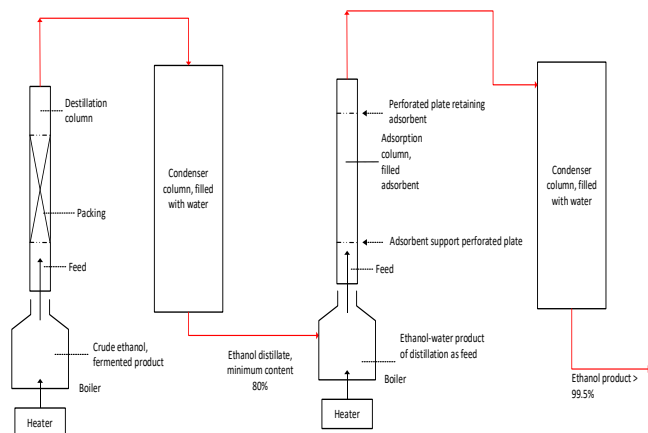


Fig. 1. Single stage distillation and adsorption equipment for ethanol purification

mL), as the result of fermentation, was fed to the distillation column. It was filled into the boiler and heated to 85 °C for 120 minutes so that the ethanol changed to the vapour phase. Furthermore, the bioethanol vapour is condensed by flowing into a spiral-shaped cooling pipe using water as a coolant. The condensate formed from the condensation process is collected in an Erlenmeyer. The sample was taken every 30 minutes for ethanol concentration analysis.

The best concentration of bioethanol from the distillation process was then used as a feed for the adsorption process containing a molecular sieve (zeolite 4A and natural zeolite) at a temperature of 90°C. Furthermore, this mixture will be reduced in water content or dehydrated. The ethanol-water vapour mixture was put into an adsorption column with an inner diameter of 8 cm and a column height of 125 cm. The variations in adsorbent height (60, 80, 100, and 120 cm) were also investigated. The adsorption process was carried out for 90 minutes, then the bioethanol was analysed.

2.9.1. Fourier transform infrared (FTIR) analysis

To qualitatively identify the presence of functional groups contained in the zeolite, a Fourier Transform Infrared (FTIR) test was carried out. Infrared spectroscopy is the method used to analyse molecular interactions with electromagnetic radiation that is in the wavenumber region 7.500 – 350 cm⁻¹.

3. Results and Discussion

3.1 Effect of bitter cassava starch concentration on glucose concentration

The effect of bitter cassava starch concentrations (150, 200, and 250 g/L) in enzyme concentrations of 1.5% (w/w) on the glucose concentration is shown in Fig. 2. The results of the hydrolysis of bitter cassava starch for 24 hours showed that the glucose concentration would increase over 3–12 hours. Further, the opposite condition occurred after 21 hours due to the decrease in glucose concentration.

The best condition was obtained at a concentration of bitter cassava starch of 200 g/L over a period of 12 hours, which resulted in a glucose concentration of 62.64%. It was due to the maximum enzyme activation (1.5%). However, other conditions (cassava starch 250 g/L) show that the enzyme concentration is not sufficient to convert starch into glucose for 18–24 hours (Hargono *et al.*, 2017b). Hargono *et al.* (2017a) also reported the

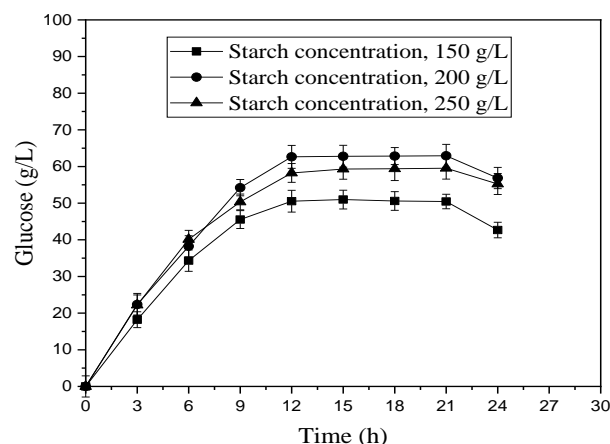


Fig. 2. The effect of bitter cassava starch concentrations in enzymes concentrations 1.5% (w/w) on the glucose concentration

reducing sugars obtained from sweet cassava starch, bitter cassava flour, and gadung flour by GSHE with a concentration of 1.5% (w/w) and a starch concentration of 200 g/L at 30 °C and pH 4 during the hydrolyzing time of 0 to 24 h (Hargono *et al.*, 2017a). The reducing sugar of sweet starch was higher than that of bitter and gadung flours. At a hydrolyzing time of 12 h, the maximum reducing sugars from sweet cassava bitter, cassava flour, and gadung flour were 40.98, 37.21, and 5.36 g/L, respectively. Previous research reported that the reducing sugar produced from cassava starch has a varying level of starch, at pH 4.5 and a temperature of 30 °C (Shanavas *et al.*, 2010). It was found that the reducing sugar of 98.3 g/L could be achieved with 100mg of starch on a 10% (w/v) starch solution. Another study also reported that the hydrolysis of native tapioca starch for 8 to 24 hours increased the reducing sugar concentration, as indicated by an increase in dextrose equivalent (DE) from 18 to 35.7% (Yusuf *et al.*, 2013). Another previous work reported that after 8 hours of hydrolysis of 30% maize starch using alpha amylase and glucoamylase, the maximum reducing sugar was 138 g/L (Adejumi *et al.*, 2009).

3.2. X-Ray diffraction pattern of hydrolyzed starch

The phases of hydrolyzed starch after the hydrolysis process with different hydrolysis times were evaluated. A characterization by XRD was carried out to determine the crystal behaviour of starch granules as an effect of enzymatic hydrolysis in the presence of cyanide inhibitors. The crystalline

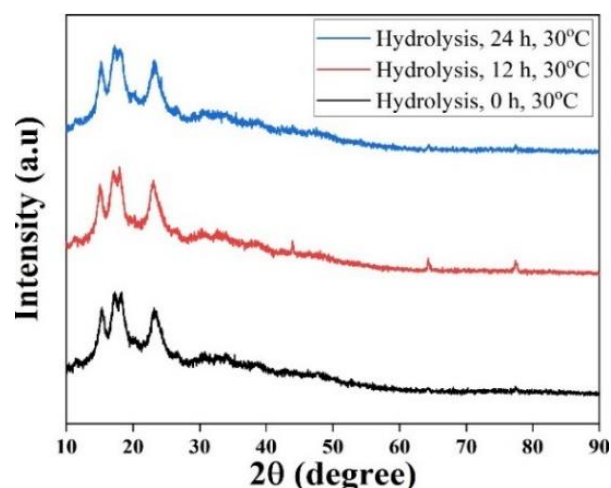


Fig. 3. XRD pattern of enzymatic hydrolysed starch

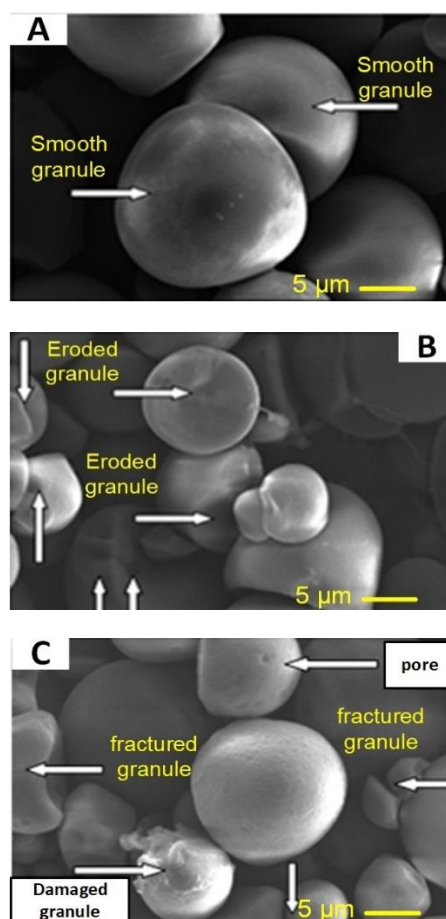


Fig 4 SEM images of starch granules at 3000x magnification (a) native bitter cassava starch, (b) hydrolyzed bitter cassava starch for 12 h, (c) hydrolyzed bitter cassava starch with for 24 h.

phase of the starch can be indicated by the presence of a sharp peak within the amorphous diffraction pattern. The XRD patterns of native bitter cassava starch and enzymatic hydrolyzed starch for 12 and 24 hours are shown in Fig. 3. The diffraction patterns of the starch are relatively similar. However, a slight, distinct pattern was identified. Naturally, starch has three types of XRD patterns: type A, type B, and type C, which represent the different crystalline structures of each starch. Both native bitter cassava starch and bitter cassava starch with hydrolysis treatment for 12 and 24 hours showed an A-type pattern with the characteristic pattern at 2θ of 15.66° and 23.32° (native starch) with peak intensities of 410 and 514 a.u. Furthermore, the XRD pattern of hydrolyzed starch for 12 hours showed typical peaks of 15.68° and 23.32° at intensities of 458 a.u. and 522 a.u., while after treatment for 24 hours, the characteristic diffraction peaks were at 2θ of 15.27° and 23.2° with intensities of 526 a.u. and 556 a.u. The crystallinity phase of native bitter starch and hydrolyzed starch for both 12 and 24 hours provided an insignificant change. The data shows that the amorphous region of the starch granules after treatment was wider than the crystalline region. Chen *et al.* (2014) reported that the intensity of hydrolyzed tapioca starch was higher than that of native tapioca starch. Cassava starch is a material that is easily hydrolyzed compared to potato starch. In accordance with this property, cassava starch and sweet potato starch show an A-type pattern. These persistent crystalline peaks of hydrolyzed starch indicated that hydrolysis mainly occurred in the amorphous region.

3.3 SEM Images of Starch Granules

SEM micrographs of native and hydrolyzed bitter cassava starch are shown in Fig. 4. The granule of native starch was regularly rounded, with an estimated size of 10 μm . The surface of the granule appeared smooth (Fig. 4a), indicating that the starch was in good condition. In contrast, the hydrolyzed starch for 12 hours (Fig. 4b) exhibited enzymatic erosion mainly on the surface, which resulted in roughening and deformation. Meanwhile, the starch hydrolysis for 24 h (Fig. 4c) shows that starch granules were cut into pieces (split), pores appeared, and some of the granules were damaged. These pieces caused a larger surface area of the granules, thus increasing the penetration of the enzyme into the starch granules during hydrolysis (Sarikaya *et al.*, 2000).

3.4. Effect of Fermentation Time on Ethanol Concentration in the SHF and SSF

The experiment data obtained from the fermentation of bitter cassava starch using SHF and SSF are shown in Fig. 5. In the initial fermentation (18 hours), the bioethanol concentration produced from SSF is lower than that from SHF. It is due to the fact that at the beginning of the fermentation, a small amount of glucose is formed, in contrast to SHF, where glucose is readily available. Fermentation of bitter cassava starch for 42 hours using the SHF and SSF methods resulted in increasing bioethanol concentrations of 12.10 and 13.82 g/L, respectively, while fermentation after 48 hours of bioethanol production tended to be constant. This result indicated that SSF is more effective than SHF. The difference in ethanol yield for 48 hours reached 14.21%. Previous research showed that fruit bunch hydrolysis could produce 6.05% bioethanol using the SSF method for 24 hours (Dahnum *et al.*, 2015). However, the SHF process could only obtain 4.74% bioethanol for 72 hours. Hargono *et al.* (2021) also reported that the hydrolysis of Suweg (*Amorphophallus campanulatus*) could produce an ethanol concentration of 99.52% by the SSF method, which was higher than the SHF method (89.57%). This method operates at low temperatures and therefore saves energy. In addition, the SSF method can inhibit excess glucose products, which can inhibit enzyme activity. In addition, SSF is carried out in one reactor to save costs (Hargono *et al.*, 2021).

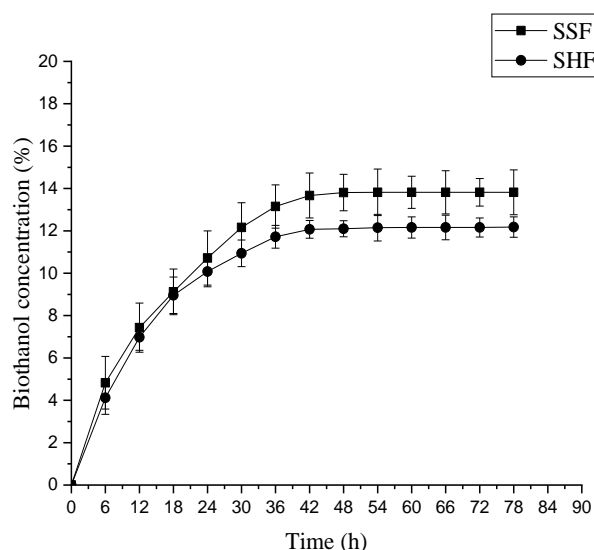


Fig 5. Effect of fermentation time on ethanol concentrations in the SHF and SSF.

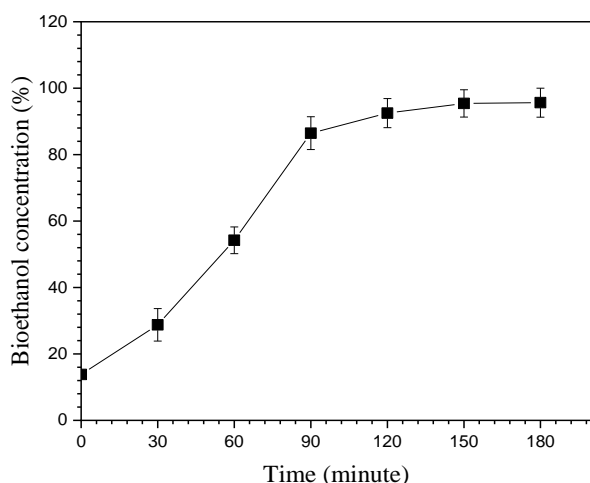


Fig 6. Effect of condensation time on bioethanol concentration

3.5. Effect of condensation time on bioethanol concentration

The effect of condensation time on the bioethanol concentration is shown in Fig. 6. As the condensation time increased from 30 to 150 minutes, the bioethanol concentration obtained increased from 28.76 to 95.42%, and the yield of bioethanol is 32.5%.

This bioethanol concentration will tend to remain due to the limitations imposed by the azeotropic point. However, in previous research carried out on the second stage of distillation from suweg (*Amorphophallus paeoniifolius*), an ethanol concentration of 91.78% was achieved after 90 minutes, after which the ethanol concentration remained constant (Hargono et al., 2021). According to Huang et al. (2008), this separation process is only able to produce a maximum ethanol concentration of 95.63% (w/w), with limitations to the azeotrope point. Other studies conducted similar research using a column with and without packing of 0.48 pore sizes. The ethanol yields obtained were, respectively, 87.5% and 62%. In a previous study, fermentation was carried out using a 5% fermented ethanol broth with a flow rate of 145 g/min, and the purification process was conducted using an integrated distillation with a membrane, resulting in an increase in ethanol concentration from 63.5 to 98.5%. (Vane et al., 2021).

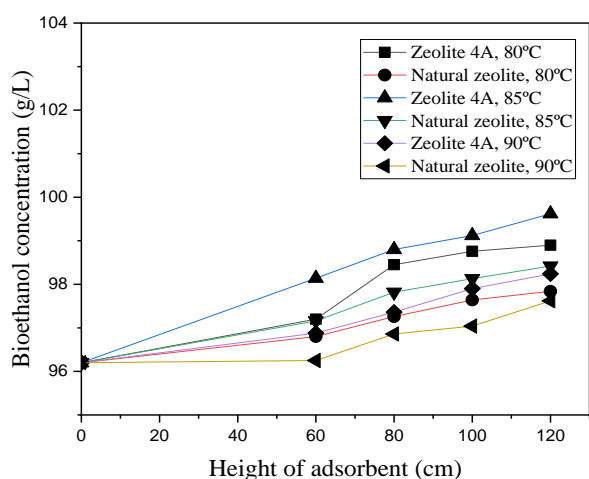


Fig 7. Effect of height adsorbent on bioethanol concentration

3.6 Effect of adsorbent height and temperature in the column on ethanol concentration

The effect of adsorbent height on ethanol concentration is shown in Fig. 7. Generally, higher temperatures and column heights significantly increased the bioethanol concentration. The best conditions were achieved at a temperature of 85°C and an adsorbent height of 120 cm. These conditions could produce ethanol concentrations of 99.62% (zeolite 4A) and 98.42% (natural zeolite) with an increase in ethanol concentration of 3.56% and 2.31%, respectively. However, the ethanol concentration only reached 2.12% and 1.48% or decreased by 1.44% and 0.83% at 90°C. Previous studies reported that the use of zeolite adsorbents could achieve an ethanol concentration of 99.40% (Handrian et al., 2017).

3.7. Fourier transform infrared test results of Zeolite 4A

Fourier Transform Infrared analysis was conducted to indicate functional groups present in Zeolite 4A. The FTIR spectra of Zeolite 4A before and after activation are shown in Fig. 8. Zeolite exhibits two main peaks in the range of 3600 and 3700 cm^{-1} . This is due to the presence of an OH group on Si-(OH-)Al located on the internal surface of the zeolite and the OH stretching from the weakly acidic silanol groups located on the external surface of the zeolite in the vibrational region of the hydroxyl stretching infrared spectrum. In the activated zeolite, the notch decreases in intensity around 3600 cm^{-1} and shifts to about 3580 cm^{-1} . The indentation near 3700 cm^{-1} is slightly weakened due to the zeolite activated by Na metal (Gackowski et al., 2019). The decrease in band intensity is most likely due to the exchange of protons with Na metal ions through the reaction:

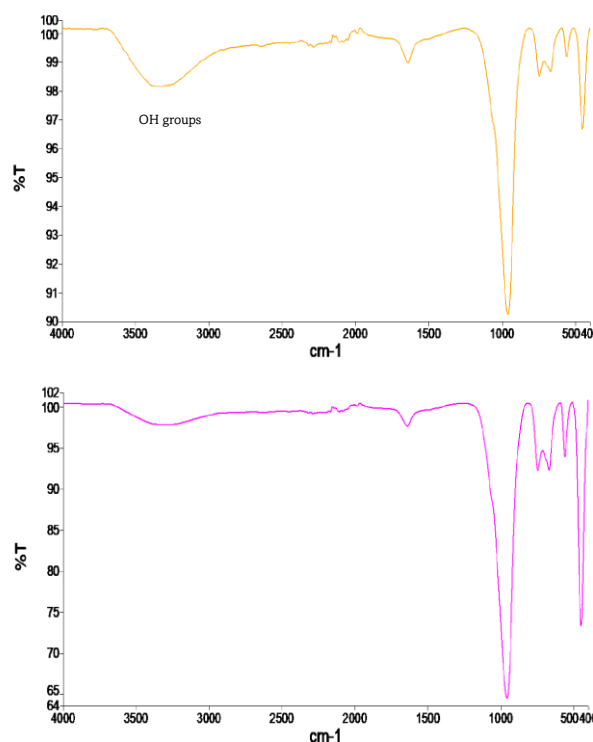
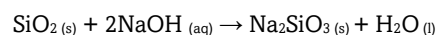


Fig 8. FTIR spectra of zeolite 4A (a) before activated and (b)

Table 1
The interpretation of wave number results in non-activated zeolite and activated zeolite

Wave Number (cm ⁻¹)			Interpretation
Non-Activated Zeolite	Activated Zeolite	Faisal <i>et al</i> (2015)	
436.05	451.58	500-420	Internal buckling vibration T-O SiO/AIO
779.49	780.19	820-650	Symmetrical stretching vibration OSiO / OAIO
1018.51	1035.63	1250-950	Asymmetric stretching vibration -OSi-O -OAl-O
1636.63	1639.23	1650-1645	Bending vibration Si-OH

The two weak bands near 1500 and 1450 cm⁻¹ in the Fourier Transform Infrared (FTIR) spectrum correspond to the Bronsted and Lewis acid sites of the zeolite. The adsorption of Na ions by zeolite leads to an increase in Al sites and a decrease in Si sites (Krol *et al.*, 2012).

3.8. Fourier transform infrared test results of natural zeolite

A Fourier Transform Infrared analysis was conducted to indicate the functional groups contained in the natural zeolite. The FTIR spectra of natural zeolite before and after activation are shown in Fig. 9. It also shows that the O-H stretching vibration from non-activated natural zeolite to activated natural zeolite has decreased. It is associated with the release of water molecules that are physically bound to the zeolite (Fitriana & Rusmini, 2019). Table 1 illustrates the interpretation of the wave number results of non-activated and activated zeolite. A decrease in absorption is observed at wave numbers between 820 and 650 cm⁻¹, which corresponds to the symmetrical

stretching vibration of OSiO/OAIO, as shown in Table 1. This vibration indicates the composition of Si-Al in the zeolite structure.

4. Conclusion

Bitter cassava (*Manihot glaziovii*) is feasible to convert into bioethanol. The simultaneous saccharification and fermentation (SSF) process resulted in bioethanol with a concentration of 13.82% (v/v). However, distillation that uses coral rock as packing material, could only purify bioethanol up to 95.64%. To further purify the bioethanol, an adsorption method was employed using zeolite 4A and natural zeolite as a continuation of the distillation process. This approach successfully increased the bioethanol concentrations of 99.62% (zeolite 4A) and 98.42% (natural zeolite). In addition, the combination method of distillation and adsorption proved to be effective in producing bioethanol of fuel-grade quality.

Acknowledgments

This research was financially supported by The Faculty of Engineering, Diponegoro University, Indonesia through Strategic Research Grant 2022.

Author Contributions: H.H.: Conceptualization, methodology, formal analysis, writing—original draft, supervision, writing—review and editing resources; NAH: project administration, writing—review and editing, project administration, S.D.A.; writing—review and editing, project administration, validation. All authors have read and agreed to the published version of the manuscript, E.W. & U.A.F.: Collecting data in this research.

Conflicts of Interest: The authors declare no conflict of interest

Funding: This research was funded by The Faculty of Engineering, Diponegoro University, Indonesia through Strategic Research Grant 2022.

References

- Abdeen, F.R.H., Mel, M., Al-Khatib, M., & Azmi, A.S. (2011). Dehydration of ethanol on zeolite based media using adsorption process. *Proceedings of the 3rd CUTSE International Conference*, 312-917.
- Adejumo, A.L., Agboola, F.K., Layokun, S.K. (2009). Hydrolysis of maize starch using amylic enzymes extracted from sorghum malt. *International Journal of Biological and Chemical Sciences*, 3(5), 1030-1041. <https://doi.org/10.4314/ijbcs.v3i5.51082>.

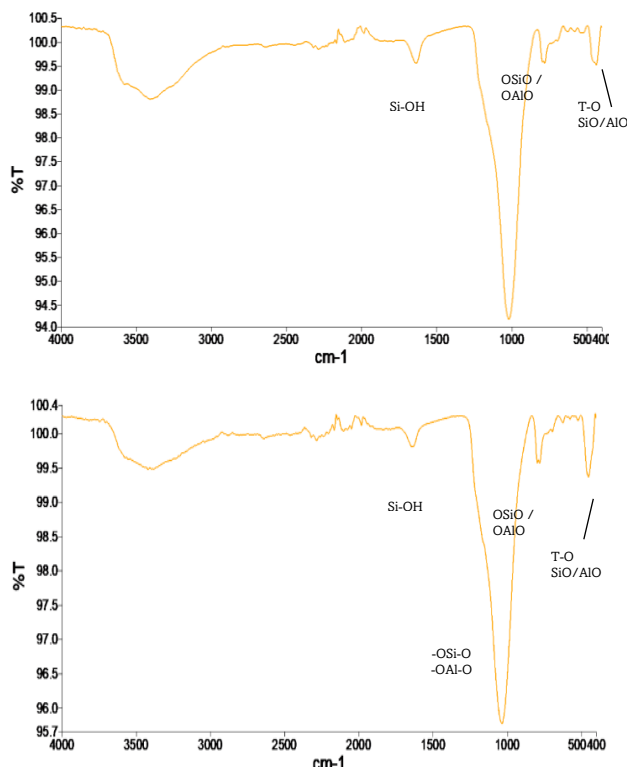


Fig 9. FTIR spectra of natural zeolite (a) before activated and (b) after activated

- Adenle, A. A., Haslam, G. E., & Lee, L. (2013). Global assessment of research and development for algae biofuel production and its potential role for sustainable development in developing countries. *Energy Policy*, 61, 182-195. <https://doi.org/10.1016/j.enpol.2013.05.088>.
- Ardiyanti, H. B., Mahlia, T. M. I., Chong, W. T., Nur, H., & Sebayang, A. H. (2016). Second generation bioethanol production: A critical review. *Renewable and Sustainable Energy Reviews*, 66, 631-653. <https://doi.org/10.1016/j.rser.2016.07.015>.
- Ardiyanti, D., and Hadiyanto, H. (2013). Ethanol production from whey by *Kluyveromyces marxianus* in batch fermentation system: Kinetics parameters estimation (2013) *Bulletin of Chemical Reaction Engineering and Catalysis*, 7 (3), 179-184. <https://doi.org/10.9767/bcrec.7.3.4044.179-184>
- Cardona, C. A., & Sánchez, Ó. J. (2007). Fuel ethanol production: process design trends and integration opportunities. *Bioresource Technology*, 98(12), 2415-2457. <https://doi.org/10.1016/j.biortech.2007.01.002>.
- Dahnum, D., Tasum, S.O., Triwahyuni, E., Nurdin, M., Abimanyu, H. (2014). Comparison of SHF and SSF processes using enzyme and dry yeast for optimization of bioethanol production from empty fruit bunch. *Energy Procedia*, 68, 107 – 116. <https://doi.org/10.1016/j.egypro.2015.03.238>.
- Delgado, J.A., Águeda, V.I., Uguina, M.A., Sotelo, J.L., García-Sanz, A., & García, A. (2015). Separation of ethanol-water liquid mixtures by adsorption on BPL activated carbon with air regeneration. *Separation and Purification Technology*, 149, 370-380. <https://doi.org/10.1016/j.seppur.2015.06.011>.
- Fitriana, N., dan Rusmini. 2019. Pembuatan Zeolit Alam Teraktivasi HCl dan Karakterisasinya. *UNESA Journal of Chemistry*, 8(1). <https://doi.org/10.26740/ujc.v8n1.p%25p>.
- Gackowski, M., Podobiński, J., Broclawik, E., & Datka, J. (2019). IR and NMR Studies of the Status of Al and Acid Sites in Desilicated Zeolite Y. *Molecules*, 25(1), 31. <https://doi.org/10.3390/molecules25010031>.
- Genencor (2009) STARGEN™ 002: Granular Starch Hydrolyzing Enzyme for Ethanol Production.
- Hadiyanto, H., Ariyanti, D., Aini, A.P., Pinundi, D.S. (2013). Batch and fed-batch fermentation system on ethanol production from whey using *Kluyveromyces marxianus*. *International Journal of Renewable Energy Development*, 2 (3), 127-131. <https://doi.org/10.14710/ijred.2.3.127-131>
- Handayani, N. A., Santosa, H., Sofyan, M., Tanjung, I., Chyntia, A., Putri, P. A. R. S., & Ramadhan, Z. R. (2013). Biodiesel production from kapok (*Ceiba pentandra*) seed oil using naturally alkaline catalyst as an effort of green energy and technology. *International Journal of Renewable Energy Development*, 2(3), 169-173. <https://doi.org/10.14710/ijred.2.3.169-173>.
- Handrian, H., Sediawan, W. B., & Mindaryani, A. (2017). Adsorpsi Air dari Campuran Uap Etanol-Air dengan Zeolit Sintetis 4A dalam Packed Bed dalam Rangka Produksi Fuel Grade Ethanol. *Jurnal Rekayasa Proses*, 11(2), 68-77. <https://doi.org/10.22146/jrekpros.30344>.
- Hargono, H., Jos, B., & Kumoro, A. C. (2017). Kinetics of the enzymatic hydrolysis of sweet cassava starch and bitter cassava flour and gadung (*Dioscorea hispida* Dennst) flour at low temperature. *Bulletin of Chemical Reaction Engineering & Catalysis*, 12(2), 256-262. <https://doi.org/10.9767/bcrec.12.2.808.256-262>.
- Hargono, H., Jos, B., & Kumoro, A. C. (2017b). Production of bioethanol from sweet and bitter cassava starches by simultaneous saccharification and fermentation using *Saccharomyces cerevisiae*. *Advanced Science Letters*, 23(3), 2427-2431. <https://doi.org/10.1166/asl.2017.8682>.
- Hargono, H., Jos, B., Purwanto, P., Sumardiono, S., Zakaria, M.F. (2021). Fuel grade bioethanol production from suweg starch through distillation-adsorption process using natural zeolite. *IOP Conf. Ser.: Mater. Sci. Eng.* 2021, 1053 012114. <https://doi.org/10.1088/1757-899X/1053/1/012090>.
- Hossain, A. B. M. S., & Fazliny, A. R. (2010). Creation of alternative energy by bio-ethanol production from pineapple waste and the usage of its properties for engine. *African Journal of Microbiology Research*, 4(9), 813-819. https://academicjournals.org/article/article1380209514_Hossain%20and%20Fazliny.pdf
- Huang, H. J., Ramaswamy, S., Tschirner, U. W., & Ramarao, B. V. (2008). A review of separation technologies in current and future biorefineries. *Separation and purification technology*, 62(1), 1-21. Adogbo GM, Ayodele AJ 2013 *International J. Sci. Eng. Res.* 4 (4) 1330- 1334. <https://doi.org/10.1016/j.seppur.2007.12.011>.
- Jambo, S. A., Abdulla, R., Azhar, S. H. M., Marbawi, H., Gansau, J. A., & Ravindra, P. (2016). A review on third generation bioethanol feedstock. *Renewable and sustainable energy reviews*, 65, 756-769. <https://doi.org/10.1016/j.rser.2016.07.064>.
- Karimi, S., Yarak, M.T., & Karri, R.R. (2019). A comprehensive review of the adsorption mechanisms and factors influencing the adsorption process from the perspective of bioethanol dehydration. *Renewable and Sustainable Reviews*, 107, 535-553. <https://doi.org/10.1016/j.rser.2019.03.025>.
- Król, M., Mozgawa, W., Jastrzębski, W., & Barczyk, K. (2012). Application of IR spectra in the studies of zeolites from D4R and D6R structural groups. *Microporous and Mesoporous Materials*, 156, 181-188. <https://doi.org/10.1016/j.micromeso.2012.02.040>.
- Kusmiyati & Susanto, H. (2015). Fuel grade bioethanol production from Iles-iles (*Amorphophalus campanulatus*) tuber. *Procedia Environmental Sciences*, 23, 199-206. <https://doi.org/10.1016/j.proenv.2015.01.031>.
- Lee, Y. H., Chen, C. H., Fazara, M. U., & Hatim, M. M. I. (2021, May). Production of fuel grade anhydrous ethanol: a review. *In IOP Conference Series: Earth and Environmental Science* (Vol. 765, No. 1, p. 012016). IOP Publishing. <https://doi.org/10.1088/1755-1315/765/1/012016>.
- Lei, Z., Wang, H., Zhou, R., & Duan, Z. (2002). Influence of salt added to solvent on extractive distillation. *Chemical Engineering Journal*, 87(2), 149-156. [https://doi.org/10.1016/S1385-8947\(01\)00211-X](https://doi.org/10.1016/S1385-8947(01)00211-X).
- Mehdi Naraki, M., Parvasi, P., Jokar, S. M., & Iulianelli, A. (2023). Experimental and theoretical feasibility study of methanol application for Echiium oil-based biodiesel production. *Renewable Energy*, 202, 1241-1247. <https://doi.org/10.1016/j.renene.2022.11.118>.
- Mekala, M., Neerudi, B., Are, P.R., Surakasi, R., Manikandan, G., Kakara, V.R., & Dhupal, A.A. (2022). Water removal from an ethanol-water mixture at azeotropic condition by adsorption technique. *Adsorption Science & Technology*, 8374471, 1-10. <https://doi.org/10.1155/2022/8374471>.
- Muhaji and Sutjahjo D H. (2018). The characteristics of bioethanol fuel made of vegetable raw materials. *IOP Conf Series, 2018: Material Science and Engineering* 296, 012019. <https://doi.org/10.1088/1757-899X/296/1/012019>.
- Nazloo, E. K., Moheimani, N. R., & Ennaceri, H. (2022). Biodiesel production from wet microalgae: Progress and challenges. *Algal Research*, 102902. <https://doi.org/10.1016/j.algal.2022.102902>.
- Ocreto, J. B., Chen, W. H., Ubando, A. T., Park, Y. K., Sharma, A. K., Ashokkumar, V., ... & De Luna, M. D. G. (2021). A critical review on second- and third-generation bioethanol production using microwaved-assisted heating (MAH) pretreatment. *Renewable and Sustainable Energy Reviews*, 152, 111679. <https://doi.org/10.1016/j.rser.2021.111679>.
- Perry, R.H., and Green, D.W., 1997, Perry's Chemical Engineers' Handbook, 7th Edition, Mc Graw-Hill Co, New York, p.1128, 1490-1497, 1534-1537.
- Pilling, M., & Holden, B. S. (2009). Choosing trays and packings for distillation. *Am. Inst. Chem. Eng. CEP*, 105, 44-50. Suali, E., & Sarbaty, R. (2012). Conversion of microalgae to biofuel. *Renewable and Sustainable Energy Reviews*, 16(6), 4316-4342. <https://doi.org/10.1016/j.rser.2012.03.047>
- Shanavas, S., Padmaja, G., Moorthy, S.N., Sajeev, M.S., Sheriff, J.T. (2010). Process Optimization for Bioethanol Production from Cassava Starch Using Novel Eco-Friendly Enzymes. *Biomass and Bioenergy*, 35: 901-909. <https://doi.org/10.1016/j.biombioe.2010.11.004>.
- Tabatabaei, M., Aghbashlo, M., Dehghani, M., Panahi, H. K. S., Mollahosseini, A., Hosseini, M., & Soufiyan, M. M. (2019). Reactor technologies for biodiesel production and processing: A review. *Progress in Energy and Combustion Science*, 74, 239-303. <https://doi.org/10.1016/j.pecs.2019.06.001>.
- Vane, L. M., Alvarez, F. R., Rosenblum, L., & Govindaswamy, S. (2013). Efficient ethanol recovery from yeast fermentation broth with integrated distillation-membrane process. *Industrial & Engineering*

Chemistry Research, 52(3),
<https://doi.org/10.1021/ie2024917>.

1033-1041.

Yussof, N. S., Utra, U., & Alias, A. K. (2013). Hydrolysis of native and cross-linked corn, tapioca, and sweet potato starches at sub-gelatinization temperature using a mixture of amylolytic enzymes. *Starch-Stärke*, 65(3-4), 285-295.
<https://doi.org/10.1002/star.201200002>



© 2023. The Author(s). This article is an open access article distributed under the terms and conditions of the Creative Commons Attribution-ShareAlike 4.0 (CC BY-SA) International License (<http://creativecommons.org/licenses/by-sa/4.0/>)